HHS Public Access

Author manuscript

Dev Dyn. Author manuscript; available in PMC 2024 May 01.

Published in final edited form as:

Dev Dyn. 2023 May ; 252(5): 589–604. doi:10.1002/dvdy.564.

Characterizing the role of Pdgfra in calvarial development

Meenakshi Umar[1], **Garrett Bartoletti**[1], **Chunmin Dong**[1], **Apurva Gahankari**[1], **Danielle Browne**[1], **Alastair Deng**[1], **Josue Jaramillo**[2], **Mimi Sammarco**[2], **Jennifer Simkin**[3], **Fenglei He**[1]

[1]Department of Cell and Molecular Biology, School of Science and Engineering, Tulane University, New Orleans, LA, United States.

[2]Department of Surgery, Tulane School of Medicine, New Orleans, LA, United States.

[3]Department of Orthopaedic Surgery, Health Sciences Center, Louisiana State University, New Orleans, LA, United States.

Abstract

Background: Mammalian calvarium is composed of flat bones developed from two origins, neural crest and mesoderm. Cells from both origins exhibit similar behavior but express distinct transcriptomes. It is intriguing to ask whether genes shared by both origins play similar or distinct roles in development. In present study, we have examined the role of *Pdgfra*, which is expressed in both neural crest and mesoderm, in specific lineages during calvarial development.

Results: We found that in calvarial progenitor cells, *Pdgfra* is needed to maintain normal proliferation and migration of neural crest cells but only proliferation of mesoderm cells. Later in calvarial osteoblasts, we found that *Pdgfra* is necessary for both proliferation and differentiation of neural crest derived cells, but not for differentiation of mesoderm derived cells. We also examined the potential interaction between Pdgfra and other signaling pathway involved in calvarial osteoblasts but did not identify significant alteration of Wnt or Hh signaling activity in *Pdgfra* genetic models.

Conclusions: Pdgfra is required for normal calvarial development in both neural crest cells and mesoderm cells, but these lineages exhibit distinct responses to alteration of Pdgfra activity.

Keywords

Pdgfra; neural crest; mesoderm; calvarial; osteoprogenitor; osteoblast; mouse

Introduction

Mammalian skull is composed of the calvarial bones, facial skeleton, and the cranial base. It is essential to protect the brain and sensory organs. Malformations in the calvarial bones can lead to craniosynostosis, dysplasia and other severe birth defects[1,2]. Understanding the

*Author for correspondence (fhe@tulane.edu).

Competing interests

The authors declare no competing or financial interests.

fundamental mechanisms of calvarial development is essential to elucidate etiologies of these diseases and to design novel therapeutic strategies.

Calvarial bones have a heterogenous origin. In mice, the calvarial vault consists of five separated bones from two distinct origins: the paired frontal bones from neural crest, the paired parietal bones from mesoderm, and one singular interparietal bone with a mixed origin contributed from both neural crest and mesoderm[3,4]. Development of the calvarial bones initiates around E9.5-E10.5 in mice, when the preosteoblasts of frontal bones and parietal bones form at the supraorbital arch (SOA) and migrate apically. From E11.5 through E13.5, the preosteoblasts within the rudiments undergo active proliferation, migration, and differentiation. By E15.5-E16.5, most of these progenitor cells differentiate into osteoblasts, and the calvarial bones expand and finally form the functional calvarial vault[5-7]. Although frontal bones and parietal bones are from different origins, they both undergo intramembranous ossification and express same genes, including those critical for embryo development and morphogenesis. Multiple growth factor signaling pathways, including Wnt, Bmp, Fgf, Hh and Pdgf signaling, have been found expressed in and important for calvarial development[6-10]. It is intriguing to ask whether these critical signaling pathways expressed in both the frontal bones and parietal bones regulates their development via same or distinct avenues.

Pdgfra encodes platelet derived growth factor receptor alpha, a receptor tyrosine kinase essential for normal embryo development and homeostasis[11]. Our previous studies show that Pdgfra and its ligands Pdgfa and Pdgfc are expressed in both the progenitors of the frontal bones and the parietal bones[10]. It is known that *Pdgfra* plays a crucial role in neural crest development[12-15], but it remains unclear whether *Pdgfra* is also required for mesoderm derived parietal bones, and how Pdgfra regulates calvarial development. *Pdgfra* genetically engineered mice provide an ideal model to illustrate these mechanisms.

In the present study, we have examined calvarial phenotypes in multiple *Pdgfra* genetic models. Our data show that neural crest and mesoderm cells respond differentially to *Pdgfra* deficiency: while in both lineages cell proliferation is decreased when *Pdgfra* is inactivated, only neural crest derived cells exhibit impaired migration. At same time, Pdgfra activation promotes migration of neural crest cells, and causes obvious phenotype in frontal bones, but has limited impact in mesoderm cell migration and parietal bone formation. Similarly, *Pdgfra* deficiency affects normal proliferation of Osx+ cells in both frontal bones and parietal bones; but only in frontal bone osteoblasts, *Pdgfra* inactivation disrupts expression of genes involved in differentiation. In conclusion, our study revealed how *Pdgfra* regulates development of frontal bones and parietal bones in distinct lineages.

Results

Pdgfra is essential for normal calvarial development

To examine the role of *Pdgfra* in calvarial development, we first analyzed the skeletal preparations of *Pdgfra* null mutant mice and $Pdgfra^{+/-}$ control. At E18.5, skeletal preparations revealed that $Pdgfra^{-/-}$ calvaria is significantly smaller than control (Fig 1a). The frontal bone area of $Pdgfra^{-/-}$ is 20.9%±7.3% (n=6, $p=1.96x10^{-8}$) of control with

significant midfacial clefting, and the parietal bone area of mutant is 43.1%± 12.4% (n=6, $p=1.18x10^{-6}$) of control (Fig 1b), showing that *Pdgfra* is essential for normal calvarial development. Next, we asked from what stage mutant mice start to develop calvarial phenotype. At E12.5-13.5, calvarial osteoblasts differentiation is detectable with alkaline phosphatase (AP) activity and marker expression, we thus analyzed the calvarial rudiments of $Pdgfra^{-/-}$ and the control at E13.5. Wholemount AP staining results showed that mutant frontal bones and parietal bones are smaller than those of the control, and the mutant phenotype is consistent at E15.5 (Fig 1c, n=4 for each phenotype). AP staining of the frontal sections showed that the frontal bone of the wildtype embryos extends apically and the edge is close to midline while the mutant frontal bone remains basal level and the edge is far from midline (Fig 1d). Similarly, the edge of the mutant parietal bone also recedes compared to the $Pdgfra^{+/-}$ control (Fig 1d). These data indicate that *Pdgfra* is essential for calvarial morphogenesis, and both frontal bones and parietal bones are affected by *Pdgfra* deficiency.

Frontal bone and parietal bone are affected differentially by Pdgfra deficiency

Lineage tracing studies revealed that the frontal bones are originated from neural crest (can be traced by *Wnt1-Cre2*) and the parietal bones are derived from mesoderm (can be traced by *Mesp1Cre*) [4,20,21]. To illustrate the role of *Pdgfra* in specific lineage, we have generated $Pdgfra^{fl/fl}$;*Wnt1-Cre2* and $Pdgfra^{fl/fl}$;*Mesp1Cre* mice, respectively. In line with previous report, most $Pdgfra^{fl/fl}$;*Wnt1-Cre2* mice exhibit perinatal lethality[12], and $Pdgfra^{fl/fl}$;*Mesp1Cre* survive postnatally and 40% beyond P15 (data not shown). Skeletal preparation showed that $Pdgfra^{fl/fl}$;*Wnt1-Cre2* mice exhibit frontal bone dysplasia (Fig 2a). The size of frontal bone of $Pdgfra^{fl/fl}$;*Wnt1-Cre2* embryos is 55.4%± 8.9% of littermate control (Fig 2b, n=8, $p=7.92x10^{-8}$), and the size of parietal bone is comparable between $Pdgfra^{fl/fl}$;*Wnt1-Cre2* and their littermate controls (Fig 2b). Skeletal preparation data showed that inactivating *Pdgfra* in the mesoderm does not alter the size of frontal bones and parietal bones at E18.5 (Fig 2c, d, n=14, p=0.50 in frontal bone, p=0.27 in parietal bone). It is also noticed that some regions of these mutant bones are transparent and thinner than littermate controls (arrows in Fig 2a, c). Micro CT surface rendering models revealed dramatic phenotype in both mutants. In $Pdgfra^{fl/fl}$;*Wnt1-Cre2*, mineralization areas in frontal bone, parietal bone and interparietal bone are smaller than littermate control (Fig 2e); while in $Pdgfra^{fl/fl}$;*Mesp1Cre* embryos, mineralization of parietal bone, interparietal bone and occipital bone is barely detected (Fig 2e). The frontal bone is still detectable in $Pdgfra^{fl/fl}$;*Mesp1Cre*, but it is also affected (Fig 2e). Virtual sections of the micro CT surface rendering models showed that mineralization of frontal bones and parietal bones are both affected in $Pdgfra^{fl/fl}$;*Wnt1-Cre2* and $Pdgfra^{fl/fl}$;*Mesp1Cre* skulls (Fig 2f). These results indicate that *Pdgfra* plays a role in the interactions between neural crest and mesoderm during calvarial development.

Examination of cell proliferation and migration in Pdgfra conditional knockout models.

During calvarial development, cell proliferation and migration are two major events of calvarial osteoprogenitors[5,6]. The phenotype of frontal bone and parietal bones in $Pdgfra^{fl/fl}$;*Wnt1-Cre2* and $Pdgfra^{fl/fl}$;*Mesp1Cre* could be caused by alteration of these events. We thus assayed both processes in *Pdgfra* conditional knockout models. At E15.5, robust Osx expression is detected in calvarial osteoprogenitors and osteoblasts.

In *Pdgfra*$^{fl/fl}$*;Wnt1-Cre2*, ratio of BrdU+/Osx+ nuclei is decreased in both frontal bone primordia (62.7%± 7.0% to littermate control, p=2.56x10^{-7}, n=3) and parietal primordia (75.3%± 16.4% to littermate control, p=5.54x10^{-3}, n=3) (Fig 3a, b). In *Pdgfra*$^{fl/fl}$*;Mesp1Cre*, BrdU+/Osx+ ratio is decreased in both frontal bones (59.0%± 13.0% to control, p=1.94x10^{-6}, n=3) and parietal bones (62.5%± 13.8% to control, p=1.88x10^{-5}, n=3) (Fig 3a, b). These results show that in vivo, *Pdgfra* deficiency in either neural crest or mesoderm affects Osx+ cell proliferation in both frontal bones and parietal bones. To dissect the role of Pdgfra in specific lineage, we have sorted primary cells from E13.5 embryonic heads of *Wnt1-Cre2;R26R*^{tdT} (neural crest cells labeled with tdT expression) and *Mesp1Cre;R26R*^{tdT} (mesoderm cells labeled with tdT expression), respectively. Pdgf-aa binds to and activates Pdgfra specifically. BrdU labeling assay results show that both neural crest cells and mesoderm cells exhibit increased cell proliferation rate by pdgf-aa treatment for 4 hours, with 1.55± 0.30 fold for neural crest cells (p=4.28x10^{-3}, n=4) and 1.61±0.28 fold for mesoderm cells (p=2.60x10^{-4}, n=4) (Fig 3c, d). After treatment with pdgf-aa treatment for 20 hours, neural crest cells still show increased cell proliferation level (1.81±0.28 fold, p=1.45x10^{-4}, n=4), but mesoderm cells proliferation rate returns to a level comparable to unstimulated control (n=4, p=0.09) (Fig 3c, d). These data show proliferation of neural crest and mesoderm cells responds differentially to pdgf-aa stimulation.

To assess the role of *Pdgfra* in cell migration, we have used primary culture of isolated frontal bone/parietal bone primordia from E14.5 embryos. Scratch assay results showed that in *Pdgfra*$^{fl/fl}$*;Wnt1-Cre2,* migration of fb primordia primary cells is reduced to 73.7% ±10.6% of littermate control (p=0.015, n=3), while that of pb primordia cells remains comparable to littermate control (97.3%±3.30% of littermate control, p=0.87, n=3) (Fig 4a, b). We observed similar trend in sorted cells from E13.5 embryonic heads of *Wnt1-Cre2;R26R*^{tdT} and *Mesp1Cre;R26R*^{tdT}: pdgf-aa stimulation for 16 hours enhances migration in neural crest cells (166.9%±32.5% of littermate control, n=3, p=8.41x10^{-5}), but not in mesoderm cells (109.6%±33.50% of littermate control, n=3, p=0.52) (Fig 4c, d). These data show Pdgfra deficiency affects neural crest derived fb primordia cell migration, and pdgf-aa treatment stimulates neural crest cell migration; while altered expression of Pdgfra or its ligand has limited effect on mesoderm cell migration. These findings also suggest that defective migration of neural crest cells and their derivatives contributes to frontal bone phenotype of *Pdgfra*$^{fl/fl}$*;Wnt1-Cre2* mice.

In addition to cell proliferation, migration, abnormal apoptosis in calvarial primordia could also cause the calvarial phenotype in Pdgfra conditional knockout models. We thus examined cleaved caspase 3 expression. Immunostaining failed to detect active apoptosis in frontal bone or parietal bone primordia of *Wnt1Cre-2* or *Mesp1Cre* conditional knockout models at E15.5 (data not shown), suggesting apoptosis is not a likely factor contributing to the calvarial phenotype.

To verify whether enhanced Pdgfra signaling affects frontal bone and parietal bone development, we have generated *Pdgfra* gain-of-function models by crossing *Pdgfra*$^{+/K}$ allele with *Wnt1-Cre2* and *Mesp1Cre* respectively. With Cre expression, *Pdgfra*$^{+/K}$ drives expression of a constitutively active form of Pdgfra from its endogenous promoter[17]. Skeletal preparations of E18.5 embryos showed that in *Pdgfra*$^{+/K}$*;Wnt1-Cre2* mice, the

frontal bones are significantly enlarged (154.4%± 19.0% of the control, $p=2.44x10^{-4}$), while the size of parietal bones remains comparable to the control(Fig 5a, b, p>0.05, n=10 for each genotype); in *Pdgfra*$^{+/K}$;*Mesp1Cre* mice, both frontal bones and parietal bones are comparable to those of littermate controls(Fig 4c, d, p=0.74 for frontal bones, p=0.07 for parietal bones, n=10 for each genotype). These results indicate that Pdgfra activation affects frontal bone development, and this is in line with above data showing *Pdgfra* promotes neural crest cell proliferation and migration (Fig 3c and 4b).

Pdgfra regulates calvarial osteoblast development

Following early calvarial morphogenesis, osteoprogenitors arrive at the presumptive sites of calvarial bones, where they continue to proliferate and differentiate into osteoblasts[5,6]. We thus asked whether *Pdgfra* regulates calvarial osteoblasts development. To this end, we generated *Pdgfra* loss-of-function and gain-of-function models using *Osx1Cre* line[18]. It was reported that *Osx1Cre* calvarial bones exhibit porous phenotype at perinatal stage[25], and our observation is in line with this report (Fig 6a). Compared to *Osx1Cre* control, the frontal bone area of *Pdgfra*$^{fl/fl}$;*Osx1Cre* is decreased to 82.6%± 5.1% (n=8, p=0.01), and the counterpart of *Pdgfra*$^{+/K}$;*Osx1Cre* is increased to 108.6%± 8.2%(n=12, p=0.044). For the parietal bone, *Pdgfra*$^{fl/fl}$;*Osx1Cre* is 78.6± 11.7% (n=8, p=0.01) of *Osx1Cre* control, and *Pdgfra*$^{+/K}$;*Osx1Cre* is 103.5%± 6.8%(n=12, p=0.29) of control (Fig 6b). Micro CT surface rendering models show that both frontal bones and parietal bones of *Pdgfra*$^{fl/fl}$;*Osx1Cre* are smaller than *Osx1Cre* control, and the mineralized area of *Pdgfra*$^{fl/fl}$;*Osx1Cre* parietal bone is decreased dramatically (Fig 6c). Virtual sections of the micro CT model show the same trend of alteration of fb and pb with change of Pdgfra activity (Fig 6d). These results show that *Pdgfra* plays an important role in Osx+ cells during formation of frontal bones and parietal bones, and Osx+ cell derived from distinct lineages might respond differentially to alteration of Pdgfra activity.

The phenotype of the *Pdgfra Osx1Cre* genetic models reflects possible alteration of apoptosis, proliferation, and differentiation in the mutants. Immunostaining with anti-cleaved caspase 3 antibody failed to detect apoptotic cells in frontal bone and parietal bone of either *Pdgfra*$^{+/fl}$;*Osx1Cre* or *Pdgfra*$^{fl/fl}$;*Osx1Cre* (data not shown). BrdU labeling results in E15.5 embryos showed that in the frontal bones, proliferation rate of *Pdgfra*$^{fl/fl}$;*Osx1Cre* osteoblasts is 64.6%± 5.9% ($p=4.84x10^{-5}$, n=3) of littermate control, and *Pdgfra*$^{+/K}$;*Osx1Cre* osteoblasts is 135.5%± 20.6%($p=1.21x10^{-3}$, n=3) of *Osx1Cre* control (Fig 7a, b); in the parietal bones, osteoblasts proliferation rate of *Pdgfra*$^{fl/fl}$;*Osx1Cre* is 56.2%± 13.5% ($p=2.08x10^{-5}$, n=3) of *Osx1Cre* control, and *Pdgfra*$^{+/K}$;*Osx1Cre* is 111.6%± 12.0% (p=0.08, n=3) of *Osx1Cre* (Fig 7a, b). These results demonstrate that *Pdgfra* is required to maintain normal osteoblast proliferation in both frontal bones and parietal bones, and activating Pdgfra increases osteoblast proliferation level in the frontal bones but not in the parietal bones. Next we analyzed gene expression required for osteoblast differentiation in these models. To this end, the frontal bones and parietal bones of E18.5 embryos have been dissected carefully then homogenized for mRNA preparation and reverse transcription. Quantitative PCR results show that expression level of *Alp* and *Ocn* are significantly decreased in *Pdgfra* deficient frontal bone osteoblasts, but expression level of other markers, including *Runx2*, *Osx*, *Col1a1* and *Opn*, was comparable to the control (Fig

7c). On the other hand, we did not observe significant change of these markers' expression in parietal bone osteoblasts of *Pdgfra*$^{fl/fl}$*;Osx1Cre*. Interestingly, none of these genes exhibits significantly differential expression level in *Pdgfra*$^{+/K}$*;Osx1* calvarial osteoblasts (Fig 7c). These results show that *Pdgfra* is important to maintain *Alp* and *Ocn* expression in frontal bone osteoblasts but not in osteoblasts of parietal bone; and Pdgfra activity augmentation does not alter calvarial osteoblasts differentiation.

Examination of crosstalk between Pdgfra and other signaling in calvarial osteoblasts

Multiple signaling pathways have been reported to regulate calvarial osteoblast development[6-9]. Of these, Hh signaling and Wnt signaling have been found important for intramembranous ossification[18,26-28]. Our previous work has shown that Pdgfra acts upstream of Wnt signaling in chondrocranial development[24].We therefore tested whether Pdgfra regulates activity of Wnt signaling and Hh signaling in calvarial osteoblasts. To this end we have isolated the frontal bones and parietal bones from *Pdgfra*$^{fl/fl}$*;Osx1Cre* and *Pdgfra*$^{+/fl}$*;Osx1Cre* control at E18.5 and prepared mRNA from the osteoblasts respectively. Quantitative PCR results showed that compared to the control, *Pdgfra*$^{fl/fl}$*;Osx1Cre* exhibits decreased *Lef1* expression in frontal bone tissues, and decreased *Axin2* and *Tcf4* expression in parietal bone tissues, while other Wnt responsive genes' expression remains comparable (Fig 8a). To verify Wnt signaling activity change, we have performed Western blot using anti-active β-catenin antibody using same tissues. As a result, no significant change of the ratio of active β-catenin against α-tubulin expression was identified in *Pdgfra*$^{fl/fl}$*;Osx1Cre* compared to *littermate Pdgfra*$^{+/fl}$*;Osx1Cre* control (Fig 8b). Similarly, no significant change was identified in expression of Hh signaling responsive genes *Gli1, Gli2, Gli3* and *Ptch1* between the mutant and control osteoblasts (Fig 8c). These results suggest that Pdgfra regulates calvarial osteoblast development either in parallel to or downstream of Wnt and Hh signaling.

Discussion

Craniofacial morphogenesis is a complicated process but cells in craniofacial skeletal tissues are predominantly derived from two origins: neural crest and mesoderm. During early development, osteoprogenitors from both origins reside in supraorbital arch (SOA), from where they both migrate apically, proliferate, and undergo intramembranous ossification. It is intriguing to ask whether gene expressed in both lineages plays a similar or distinct role in these two cell types. Our data support the latter. Pdgfra and its ligands are co-expressed in both frontal bones and parietal bones[10]. Genetically engineered *Pdgfra* alleles thus provide an ideal model to study the role of same gene in these two cell types in vivo. In the present study, we found that *Pdgfra* is essential for both neural crest cells and mesoderm cells but plays distinct roles: in neural crest cells, *Pdgfra* regulates cell proliferation and migration; while in mesoderm cells, *Pdgfra* is essential to maintain cell proliferation rate but not required for cell migration. At later stages of calvarial osteogenesis, *Pdgfra* also play overlapping but distinct role in osteoblasts from two origins: in neural crest-derived osteoblasts it is essential for both proliferation and differentiation but in mesoderm-derived osteoblasts it is only required for cell proliferation. These conclusions are also supported

by our data showing distinct calvarial bone phenotypes of corresponding mouse models summarized in Fig 8a, b.

Differential response of NCCs and mesoderm cells towards same genetic factor regulation

The differential behavior of neural crest cells and mesoderm cells has also been studied by other groups. In line with our findings, these works identified difference between osteoblasts from mouse embryonic frontal bone and parietal bone. Hu and colleagues have sequenced and compared transcriptome of E17.5 mouse embryonic frontal bones and parietal bones. It has been found that 325 genes show differential expression level. Gene ontology analysis revealed that genes with higher expression level in frontal bone are closely related to proliferation and self-renewal, while those expressed preferably in parietal bone are related to extracellular matrix and anti-proliferation[29]. In another study, Li and colleagues found that frontal bone osteoblasts isolated from E17.5 mouse embryonic calvaria exhibit greater proliferation rate and osteogenic capacity than those from parietal bones, and such differences are correlated with differential FGF signaling activity[30]. While both studies provide important information to understand the difference of frontal bone and parietal bone osteoblasts, it remains unclear whether these differences exist before E17.5, and how calvarial osteoprogenitor cells from different origin develop in vivo. In this study we have used various genetic models to dissect the role of *Pdgfra* in both lineages. The calvarial phenotypes of these models illustrate Pdgfra activity alteration on calvarial development. Our data revealed that *Pdgfra deficiency* in *Wnt1Cre-2* lineage or *Mesp1Cre* lineage decreases cell proliferation rate of Osx+ cells derived from both lineages (Fig 3), but only affect cell migration of neural crest derived calvarial osteoprogenitor/osteoblasts (Fig 4). Similarly, in cells expressing *Osx1Cre*, *Pdgfra* deficiency decreases cell proliferation rate in both frontal bones and parietal bones, but only affects osteoblast differentiation marker expression in frontal bone (Fig 7). These data indicate that *Pdgfra* is required to maintain normal cell proliferation rate of calvarial osteoblasts derived from both neural crest and mesoderm, and *Pdgfra* seems only needed for migration and differentiation of neural crest derived cells, but not for those from mesoderm.

Tissue-tissue interaction during calvarial development

An interesting observation we made in this study is the frontal bone phenotype of $Pdgfra^{fl/fl};Mesp1Cre$ (Fig 2e, f). *Mesp1Cre* knock-in allele drives Cre expression exclusively in mesoderm cells[21]. So, how does inactivating *Pdgfra* in mesoderm cells cause defect in frontal bones derived from neural crest cells? BrdU labeling results also confirmed that proliferation rate of $Pdgfra^{fl/fl};Mesp1Cre$ frontal bone osteoblasts is decreased (Fig 2f). We thus have re-examined the expression pattern of *Mesp1Cre* in the developing calvaria. X-gal staining of $Mesp1Cre;R26R^{LacZ}$ and $Wnt1Cre\text{-}2;\ R26R^{LacZ}$ reveals that at E16.5, *LacZ* expression in these two lines exhibits a complementary pattern, and the frontal bone rudiment is populated from neural crest derived cells (data not shown), consistent with previous report[4]. However, the frontal bone is sandwiched by mesoderm derived mesenchymal cells and meninges (data not shown). Since tissue-tissue interaction is a

common mechanism that underlying organogenesis, one possible scenario is that closely juxtaposed mesoderm cells might affect proliferation of adjacent frontal bone cells. Our data also suggest that *Pdgfra* plays a role in this tissue-tissue interaction. From our lineage tracing data, we also noticed few neural crest derived cells in parietal bone, and vice versa (data not shown). These data show that the frontal bone cells are not exclusively derived from the neural crest and that the parietal bone are not only derived of the mesoderm. Different from the dogmatic model, the frontal bones are originated from both the neural crest and mesoderm, with neural crest contributes predominantly. The frontal bone defects of *Pdgfra*$^{fl/fl}$*;Mesp1Cre* thus could be caused by Pdgfra deficiency of the few mesoderm-derived cells within the frontal bone. It would be an intriguing question to ask what the function of these mesoderm cells during frontal bone development is. In summary, the mechanisms underlying the frontal bone defect of *Pdgfra*$^{fl/fl}$*;Mesp1Cre* mice could lie in either of above mechanisms: tissue-tissue interaction, direct regulation, or a combination of both.

The role of *Pdgfra* in osteoblasts

Pdgfra plays important roles in development and disease[11,31], but the mechanisms of its regulation on bone formation and osteoblasts still remain to be elucidated. Recent studies have highlighted its function in these aspects using various models. *PDGFRA* is found expressed in human and mouse osteoblasts, and controls bone resorption together with Pdgfrb[32]. In mesenchymal stem cells, PDGF-AA stimulation promotes osteogenic differentiation and migration[33]. Increased expression level and activity of PDGFRA and EGFR were also found correlated with abnormal differentiation of calvarial osteoblasts in patients with Apert syndrome[34]. In another study, Moenning et al., has generated a Pdgfra gain-of-function mouse model by expressing human PDGFRA D846V cDNA[35]. It was found that expression of this constitutively activated *PDGFRA* allele in neural crest causes enhanced proliferation of frontal bone osteoprogenitors as well as accelerated ossification of osteoblasts[35]. These results are in line with our observation that Pdgfra activation in neural crest cells promotes proliferation and caused enlarged frontal bones (Fig3, 5a).

In *Pdgfra*$^{fl/fl}$*;Osx1Cre* models, micro CT scanning revealed that mineralized area of parietal bones is severely affected (Fig 6c), but expression of osteoblast differentiation markers in these bones remains comparable to the control (Fig 7c). A possible explanation is that with *Pdgfra* deficiency caused proliferation reduction, osteoblasts population is severely declined (Fig 7a, b). Although differentiation and secretion of extracellular matrix of each osteoblast are not disrupted, these bones still exhibit reduced mineralization.

Crosstalk between Pdgfra and other signaling pathways in calvarial development

Signaling crosstalk provide a fine tuning of development and homeostasis. In our previous report, it is found that *Pdgfra* regulates mesoderm derived embryonic mesenchymal stem cells differentiation towards chondrocytes by inhibiting Wnt/beta-catenin signaling[24]. In this work, we found that *Pdgfra* deficiency decreases expression level of some Wnt signaling target genes (Fig 8a), but expression of active β-catenin remains comparable in

the same cells (Fig 8b). These data suggest that Pdgfra might regulates *Lef1, Tcf4* and *Axin2* expression in a β-catenin independent manner. In addition, unlike in embryonic mesenchymal stem cells, *Wnt9a* expression is not affected by alteration of Pdgfra activity[24] in calvarial osteoblasts (Fig 8a). These results indicate crosstalk between Pdgfra and Wnt signaling might be cell-context dependent.

In addition to Wnt and Hh signaling, Bmp and Fgf signaling are also implicated in calvarial development. Deletion of *Bmpr1a* in neural crest cells disrupts frontal bone development by inducing apoptosis[36], while augmented Bmp1a activity leads to hypertelorism, increased distance between eyes, suggesting a potential phenotype of frontal bones[37]. Inactivation of Bmp signaling target genes *Msx1* and *Msx2* in neural crest cells also causes frontal bone defect, accompanied with defects in differentiation and proliferation of osteogenic cells[38, 39]. Fgf receptors are receptor tyrosine kinases like Pdgfrs, and Fgfr2 sharing many downstream signaling pathways with Pdgfra in neural crest cells[40]. Inactivating Fgfr1 and Fgfr2 in neural crest cells leads to dramatic midfacial clefting and frontal bone defect[41]. On the other hand, augmented Fgfr2 activity (as in $Fgfr2^{S252W}$ allele) in neural crest cells and mesoderm cells, causes deformed frontal bones and parietal bones, accompanied by decreased cell proliferation in calvarial osteoblasts[42]. These phenotypes are distinct from those caused by Pdgfra activation in our $Pdgfra^{+/K}$ models (Fig 5), suggesting that excessive activity of Fgfr2 and Pdgfra may take different avenues to regulate calvarial development.

Experimental Procedures

Mice

All animal studies were performed according to the protocol approved by the Institutional Animal Care and Use Committee of Tulane University. The following mouse lines were maintained on a C57BL/6J background: $Pdgfra^{tm11(EGFP)Sor}$ [16], referred to as $Pdgfra^{+/-}$, $Pdgfra^{tm12Sor}$ [17], referred to as $Pdgfra^{+/K}$, *Tg (Sp7-tTA,tetO-EGFP/cre)*$^{1Amc/J}$ referred to as *Osx1Cre*[18], and *Gt(ROSA)26 Sor*$^{tm9(CAG-tdTomato)Hze}$ [19], referred to as $R26R^{tdT}$. All other mice strain including $Pdgfra^{tm8Sor}$ [15], referred to as $Pdgfra^{+/fl}$, $E2f1^{Tg(Wnt1-cre)2Sor}$ [20], referred to as *Wnt1Cre-2*, and $Mesp1^{tm2(cre)Ysa}$ [21] ,referred to as *Mesp1Cre,* were maintained on a mixed *C57BL/ 6J; 129SvJaeSor* background. The vaginal plug was checked daily in the mating females, and the midday when vaginal plug was observed was considered as embryonic day (E) 0.5.

Histology and Alkaline Phosphatase-Alcian Blue (AP-AB) staining

Embryos were dissected in ice cold PBS, and the embryonic head samples were washed and fixed in 4% paraformaldehyde (PFA)/PBS overnight at 4°C. Following gradient ethanol washes, samples were cleared in histoclear and embedded in paraffin for sectioning. AP-AB staining was performed as described previously[22].

Skeletal preparation

Skeletal preparation was performed as described previously[23]. In short, E18.5 embryos were dissected in PBS. Following removal of skin and evisceration, they were fixed in 95% ethanol for overnight at room temperature. Samples were then stained in alizarin red/ alcian

blue staining solution (0.005% alizarin red, 0.015% alcian blue and 5% glacial acetic acid in 70% ethanol) at 37°C for 3 days. Stained samples were then rinsed in 95% ethanol and then cleared in 1% KOH solution overnight. The samples were then further cleared in gradients of glycerol/KOH solutions (20%, 40%, 60%, 80%) and finally stored in 80% glycerol/KOH solution.

Primary cell culture and scratch assay

The mesenchymal cells from neural crest or mesoderm cells were isolated from E13.5 embryonic heads as described previously[24]. Briefly, calvarial tissues above eyes of E13.5 embryos was carefully dissected from *Wnt1Cre-2;R26R*^{tdT} or *Mesp1Cre;R26R*^{tdT}, respectively. With removal of brain, dura and ectoderm, mesenchymal cells expressing tdTomato were sorted and collected in MEM alpha medium supplemented with 20% Fetal Bovine Serum (FBS), 100 U/ml penicillin, 100 μg/ml streptomycin (Gibco, 15140122) and 10 mM HEPES (Millipore, TMS-003-C). Sorted cells were cultured and passed in DMEM media supplemented with 10% FBS, 100 U/ml penicillin and 100 ug/ml streptomycin.

The scratch assay was performed as described previously[12]. For in vitro assay, sorted cells of passage 2 were plated in 6 well plate and starved with 0.1% FBS for 24 hours after reaching 70-80% confluency. Scratches were created using sterile 200 ul pipette tip. Following scratch formation, cells were immediately treated with 30 ng/ml of pdgf-aa (R&D systems, 221-AA) or 0.1% FBS for 16 hours. Areas covered by cells were quantified and subject to statistical analysis. For in vivo assay, frontal bone primordia and parietal bone primordia were dissected from E14.5 embryos and dissociated using 0.125% Trypsin-EDTA (VWR, 45000-664) in PBS at 37°C for 10 min. Trypsin-EDTA was then neutralized with DMEM medium with 10% serum at 1:1 ratio. Cells were cultured in DMEM media (Gibco, 11885084) supplemented with 10% FBS (Gibco, 10438026), 100 U/ml penicillin and 100 μg/ml streptomycin (Gibco, 15140122). Scratches were created using sterile 200 ul pipette tips and areas covered by cells were imaged at 0 hour and 16 hours for quantification and statistical analysis. Statistical data are presented as mean ±SEM, and subjected to double tailed Student's *t*-tests.

Micro CT scanning

Ex vivo micro CT mages were generated using a Skyscan 1172 (Bruker, Kontich, Belgium) at 2K resolution and a pixel size of 7.87 μm with energy and intensity settings at 52 kV and 193 μA for E18.5 murine skulls. Micro CT images were captured at a rotation angle of 0.4 for E18.5 skulls with a frame averaging of 5, sample rotation at 360° and low-energy X-ray filtration using a 0.25 mm aluminum filter. Raw images were processed on NRecon and surface rendered models were generated using the volume-rendering software CTvox.

BrdU labeling and immunofluorescence staining

For in vivo assay, pregnant female mice with E15.5 embryos were administered with BrdU (50 ug/g of body weight) via intraperitoneal injection. 1 hour later, embryonic heads were dissected in ice cold PBS then fixed in fixative (2% formaldehyde and 0.2% glutaraldehyde in PBS) at 4°C overnight. Samples were then dehydrated in gradient washes of sucrose and embedded in OCT. The immunofluorescence staining was performed as described

previously[24]. Following primary antibodies were used: anti-GFP (Aves Labs, 1020, 1:800), anti-sp7(Osx) (Sigma, AV3162, 1:200), anti-cleaved caspase 3 (Cell Signaling Technology, 9661, 1:400), and anti-BrdU (Novus, NBP2-14890, 1:200). Secondary antibodies include Alexa fluor 594 (Thermo Fisher, A11012, 1:400) or Alexa fluor 488 (Thermo Fisher, A11039, 1:400). For in vitro BrdU labeling, sorted cells were seeded on glass coverslips, and incubated with 10 ug/ml BrdU for 30 minutes. Subsequently, the cells were washed in PBS, fixed in 4% PFA for 10 minutes and then incubated in 1N HCl for 10 minutes. Immunofluorescence assay using anti-BrdU antibody was performed as described above.

Quantitative real-time PCR (qRT-PCR)

Paired frontal bone and parietal bone were carefully dissected from E18.5 wild type and mutant embryos. Periosteum and dura mater from frontal and parietal bones were meticulously removed and total RNA were isolated using TRIZOL reagent (Invitrogen, 15596026). 1 ug RNA of each sample was used for 20 ul cDNA synthesis using iScript™ cDNA Synthesis kit (Bio-Rad laboratories, 1708891). 2 ul of diluted cDNA sample (1:5 in dH_2O) was used for PCR reaction. qRT-PCR was performed on Bio-Rad iCycler using SYBR Green PCR Master Mix (Applied Biosystem, 4364346). The following amplifications conditions were used: 95 °C for 10 min, followed by 40 cycles of 95 °C for 15 sec and 60 °C for 1 min. Each gene's cycle threshold (Ct) values were normalized to the β-actin.

Western blot

For each lysate sample, frontal bones and parietal bones were carefully dissected and isolated from E18.5 embryos. Genotyped samples were homogenized and pooled in RIPA buffer with protease inhibitor cocktail (Roche, 11836153001). Protein concentration was determined using Pierce BCA Protein Assay Kit (Thermo Fisher Scientific, 23225). Immunoblotting was performed following standard protocol using following primary antibodies: anti-active β-Catenin (Cell Signaling Technology, D13A1, 1:1000) and anti-α-Tubulin antibody (Millipore Sigma, 05-829, 1:1000). Secondary antibodies include IRDye 680RD (926–68070) and 800CW (926–32211) from LI-COR Biosciences. The Odyssey CLx Imaging System (LI-COR Biotechnology) and Image Studio software (LI-COR Biotechnology) were used for visualization of immunoblot and quantification.

X-gal staining

X-gal staining was performed following standard protocol. Briefly, E15.5 embryos were collected in ice cold PBS and embedded in OCT following gradient sucrose dehydration. Cryosections of 12 um were obtained at the level of coronal suture. The slides were washed in PBS and then incubated in staining solution containing 0.4 mg/ml X-gal, 5 mM potassium ferricyanide, 5 mM potassium ferrocyanide, 2 mM MgCI2, 0.01% sodium deoxycholate, and 0.02% Nonidet P-40 (NP-40) in PBS for overnight at room temperature. Following color development, slides were washed in PBS and counterstained with 0.1% nuclear fast red (Acros Organics, 211980050) and mounted for imaging.

Acknowledgements

We thank Emily Orsino and Gerrit Holleman for their excellent genotyping work. We are grateful to our lab colleagues for their critical and constructive comments.

Funding

This work was supported by Tulane University and NIH/National Institute of Dental and Craniofacial Research grant DE028918 to F.H.

References

1. Morriss-Kay GM, Wilkie AO. Growth of the normal skull vault and its alteration in craniosynostosis: insights from human genetics and experimental studies. J Anat. Nov 2005;207(5):637–53. [PubMed: 16313397]
2. Wilkie AO. Craniosynostosis: genes and mechanisms. Hum Mol Genet. 1997;6(10):1647–56. [PubMed: 9300656]
3. Jiang X, Iseki S, Maxson RE, Sucov HM, Morriss-Kay GM. Tissue origins and interactions in the mammalian skull vault. Dev Biol. 2002;241(1):106–116. [PubMed: 11784098]
4. Yoshida T, Vivatbutsiri P, Morriss-Kay G, Saga Y, Iseki S. Cell lineage in mammalian craniofacial mesenchyme. Mech Dev. 2008;125(9–10):797–808. [PubMed: 18617001]
5. Deckelbaum RA, Holmes G, Zhao Z, Tong C, Basilico C, Loomis CA. Regulation of cranial morphogenesis and cell fate at the neural crest-mesoderm boundary by engrailed 1. Development. Apr 2012;139(7):1346–58. [PubMed: 22395741]
6. Ferguson JW, Atit RP. A tale of two cities: The genetic mechanisms governing calvarial bone development. Genesis. Jan 2019;57(1):e23248. [PubMed: 30155972]
7. Ishii M, Sun J, Ting MC, Maxson RE. The Development of the Calvarial Bones and Sutures and the Pathophysiology of Craniosynostosis. Curr Top Dev Biol. 2015;115:131–56. [PubMed: 26589924]
8. Cong Q, Xu R, Yang Y. Gα(s) signaling in skeletal development, homeostasis and diseases. Curr Top Dev Biol. 2019;133:281–307. [PubMed: 30902256]
9. Gou Y, Zhang T, Xu J. Transcription Factors in Craniofacial Development: From Receptor Signaling to Transcriptional and Epigenetic Regulation. Curr Top Dev Biol. 2015;115:377–410. 10.1016/bs.ctdb.2015.07.009. [PubMed: 26589933]
10. He F, Soriano P. Dysregulated PDGFRalpha signaling alters coronal suture morphogenesis and leads to craniosynostosis through endochondral ossification. Development. Nov 1 2017;144(21):4026–4036. [PubMed: 28947535]
11. Andrae J, Gallini R, Betsholtz C. Role of platelet-derived growth factors in physiology and medicine. Genes Dev. 2008;22(10):1276–1312. [PubMed: 18483217]
12. He F, Soriano P. A critical role for PDGFRalpha signaling in medial nasal process development. PLoS Genet. 2013;9(9):e1003851. 10.1371/journal.pgen.1003851. [PubMed: 24086166]
13. Mo J, Long R, Fantauzzo KA. Pdgfra and Pdgfrb Genetically Interact in the Murine Neural Crest Cell Lineage to Regulate Migration and Proliferation. Front Physiol. 2020;11:588901. [PubMed: 33224039]
14. Smith CL, Tallquist MD. PDGF function in diverse neural crest cell populations. Cell Adh Migr. Oct-Dec 2010;4(4):561–6. [PubMed: 20657170]
15. Tallquist MD, Soriano P. Cell autonomous requirement for PDGFR in populations of cranial and cardiac neural crest cells. Development. 2003;130(3):507–518. [PubMed: 12490557]
16. Hamilton TG, Klinghoffer RA, Corrin PD, Soriano P. Evolutionary Divergence of Platelet-Derived Growth Factor Alpha Receptor Signaling Mechanisms. Mol Cell Biol. June 1, 2003 2003;23(11):4013–4025. [PubMed: 12748302]
17. Olson LE, Soriano P. Increased PDGFRalpha activation disrupts connective tissue development and drives systemic fibrosis. Dev Cell. Feb 2009;16(2):303–13. [PubMed: 19217431]

18. Rodda SJ, McMahon AP. Distinct roles for Hedgehog and canonical Wnt signaling in specification, differentiation and maintenance of osteoblast progenitors. Development. Aug 2006;133(16):3231–44. [PubMed: 16854976]
19. Madisen L, Zwingman TA, Sunkin SM, et al. A robust and high-throughput Cre reporting and characterization system for the whole mouse brain. Nat Neurosci. Jan 2010;13(1):133–40. [PubMed: 20023653]
20. Lewis AE, Vasudevan HN, O'Neill AK, Soriano P, Bush JO. The widely used Wnt1-Cre transgene causes developmental phenotypes by ectopic activation of Wnt signaling. Dev Biol. Jul 15 2013;379(2):229–34. [PubMed: 23648512]
21. Saga Y, Miyagawa-Tomita S, Takagi A, Kitajima S, Miyazaki J, Inoue T. MesP1 is expressed in the heart precursor cells and required for the formation of a single heart tube. Development. Aug 1999;126(15):3437–47. [PubMed: 10393122]
22. Dong C, Umar M, Bartoletti G, Gahankari A, Fidelak L, He F. Expression pattern of Kmt2d in murine craniofacial tissues. Gene Expr Patterns. Dec 2019;34:119060. [PubMed: 31228576]
23. Yang T, Moore M, He F. Pten regulates neural crest proliferation and differentiation during mouse craniofacial development. Dev Dyn. Feb 2018;247(2):304–314. [PubMed: 29115005]
24. Bartoletti G, Dong C, Umar M, He F. Pdgfra regulates multipotent cell differentiation towards chondrocytes via inhibiting Wnt9a/beta-catenin pathway during chondrocranial cartilage development. Dev Biol. Oct 1 2020;466(1-2):36–46. [PubMed: 32800757]
25. Wang L, Mishina Y, Liu F. Osterix-Cre transgene causes craniofacial bone development defect. Calcif Tissue Int. Feb 2015;96(2):129–37. [PubMed: 25550101]
26. Goodrich LV, Johnson RL, Milenkovic L, McMahon JA, Scott MP. Conservation of the hedgehog/patched signaling pathway from flies to mice: induction of a mouse patched gene by Hedgehog. Genes Dev. February 1, 1996;10(3):301–312. [PubMed: 8595881]
27. He X, Zhang L, Chen Y, et al. The G protein α subunit Gαs is a tumor suppressor in Sonic hedgehog-driven medulloblastoma. Nat Med. Sep 2014;20(9):1035–42. [PubMed: 25150496]
28. Mak KK, Chen MH, Day TF, Chuang PT, Yang Y. Wnt/beta-catenin signaling interacts differentially with Ihh signaling in controlling endochondral bone and synovial joint formation. Development. Sep 2006;133(18):3695–707. [PubMed: 16936073]
29. Hu B, Wu T, Zhao Y, Xu G, Shen R, Chen G. Physiological Signatures of Dual Embryonic Origins in Mouse Skull Vault. Cell Physiol Biochem. 2017;43(6):2525–2534. [PubMed: 29130970]
30. Li S, Quarto N, Longaker MT. Activation of FGF Signaling Mediates Proliferative and Osteogenic Differences between Neural Crest Derived Frontal and Mesoderm Parietal Derived Bone. PLoS ONE. 2010;5(11):e14033. [PubMed: 21124973]
31. Caplan AI, Correa D. PDGF in bone formation and regeneration: new insights into a novel mechanism involving MSCs. J Orthop Res. Dec 2011;29(12):1795–803. [PubMed: 21618276]
32. Brun J, Andreasen CM, Ejersted C, Andersen TL, Caverzasio J, Thouverey C. PDGF Receptor Signaling in Osteoblast Lineage Cells Controls Bone Resorption Through Upregulation of Csf1 Expression. J Bone Miner Res. Dec 2020;35(12):2458–2469. [PubMed: 32777109]
33. Li A, Xia X, Yeh J, et al. PDGF-AA promotes osteogenic differentiation and migration of mesenchymal stem cell by down-regulating PDGFRalpha and derepressing BMP-Smad1/5/8 signaling. PLoS ONE. 2014;9(12):e113785. [PubMed: 25470749]
34. Miraoui H, Ringe J, Haupl T, Marie PJ. Increased EFG- and PDGFalpha-receptor signaling by mutant FGF-receptor 2 contributes to osteoblast dysfunction in Apert craniosynostosis. Hum Mol Genet. May 1 2010;19(9):1678–89. [PubMed: 20124286]
35. Moenning A, Jager R, Egert A, Kress W, Wardelmann E, Schorle H. Sustained platelet-derived growth factor receptor alpha signaling in osteoblasts results in craniosynostosis by overactivating the phospholipase C-gamma pathway. Mol Cell Biol. Feb 2009;29(3):881–91. [PubMed: 19047372]
36. Saito H, Yamamura K, Suzuki N. Reduced bone morphogenetic protein receptor type 1A signaling in neural-crest-derived cells causes facial dysmorphism. Dis Model Mech. Nov 2012;5(6):948–55. [PubMed: 22773757]

37. Hayano S, Komatsu Y, Pan H, Mishina Y. Augmented BMP signaling in the neural crest inhibits nasal cartilage morphogenesis by inducing p53-mediated apoptosis. Development. Apr 1 2015;142(7):1357–67. [PubMed: 25742798]

38. Han J, Ishii M, Bringas P Jr., Maas RL, Maxson RE Jr., Chai Y. Concerted action of Msx1 and Msx2 in regulating cranial neural crest cell differentiation during frontal bone development. Mech Dev. Sep-Oct 2007;124(9-10):729–45. [PubMed: 17693062]

39. Ishii M, Merrill AE, Chan YS, et al. Msx2 and Twist cooperatively control the development of the neural crest-derived skeletogenic mesenchyme of the murine skull vault. Development. Dec 2003;130(24):6131–42. [PubMed: 14597577]

40. Vasudevan HN, Mazot P, He F, Soriano P. Receptor tyrosine kinases modulate distinct transcriptional programs by differential usage of intracellular pathways. Elife. 2015;4. 10.7554/eLife.07186.

41. Ray AT, Mazot P, Brewer JR, Catela C, Dinsmore CJ, Soriano P. FGF signaling regulates development by processes beyond canonical pathways. Genes Dev. Dec 1 2020;34(23-24):1735–1752. [PubMed: 33184218]

42. Holmes G, Basilico C. Mesodermal expression of Fgfr2S252W is necessary and sufficient to induce craniosynostosis in a mouse model of Apert syndrome. Dev Biol. Aug 15 2012;368(2):283–93. [PubMed: 22664175]

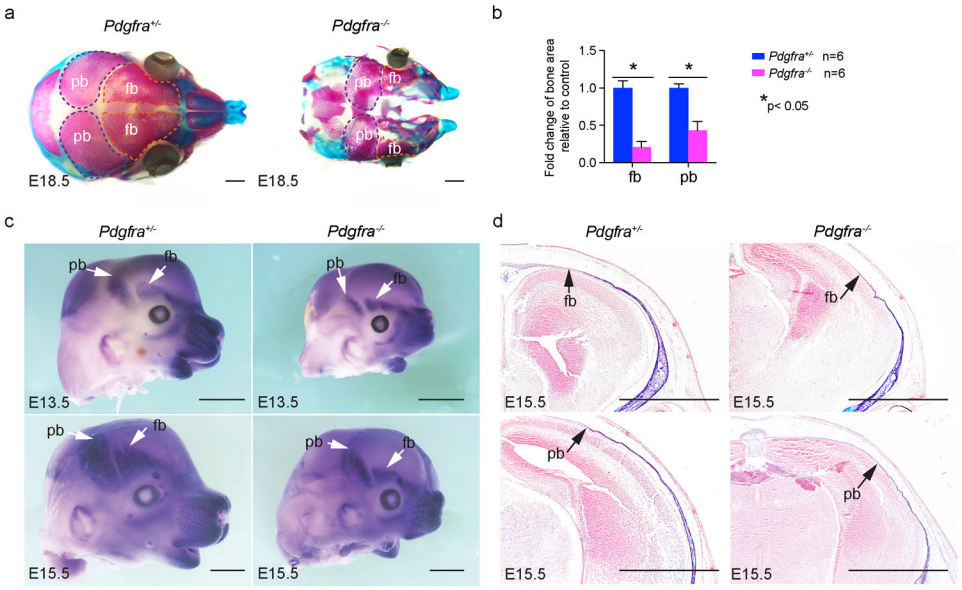

Figure 1. Pdgfra is required for normal calvarial development

(a) Skeletal preparation of *Pdgfra*$^{+/-}$ and *Pdgfra*$^{-/-}$ at E18.5 (top view). Frontal bones and parietal bones are outlined with dashed lines. (b) Quantification of area of fb and pb in a. (c) Wholemount AP staining of *Pdgfra*$^{+/-}$ and *Pdgfra*$^{-/-}$ at E13.5 and E15.5. Blank arrows point to fb and pb (side view). (d) AP staining on coronal sections of *Pdgfra*$^{+/-}$ and *Pdgfra*$^{-/-}$ at E15.5 counterstained with NFR, with arrows pointing to edge of fb or pb. fb, frontal bone; pb, parietal bone. Scale bar = 1mm.

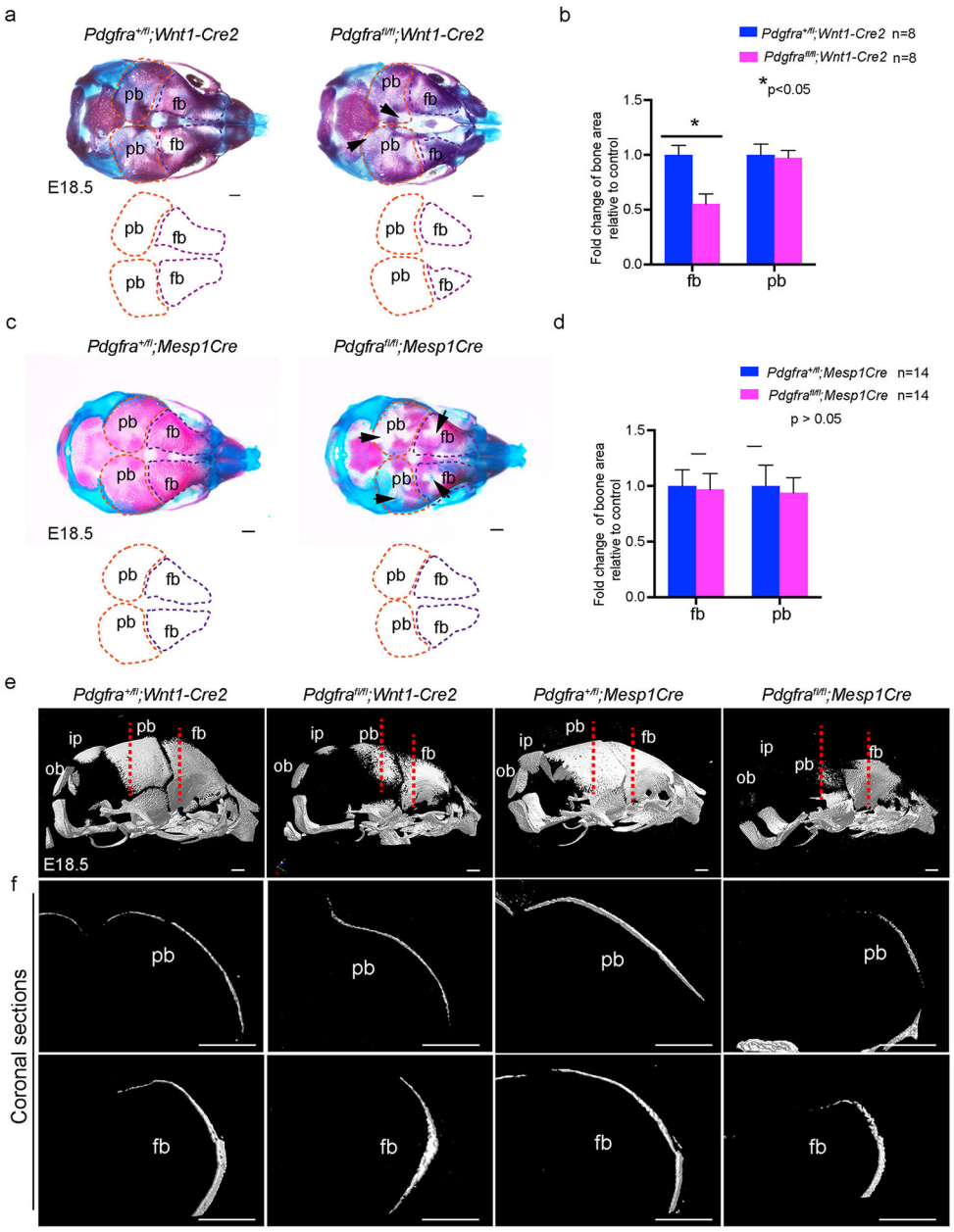

Figure 2. Calvarial phenotypes caused by inactivating *Pdgfra* in specific lineage.

(a) Skeletal preparation of *Pdgfra*$^{+/fl}$;*Wnt1-Cre2* and *Pdgfra*$^{fl/fl}$;*Wnt1-Cre2* at E18.5 (top view). Dashed lines outline fb and pb. (b) Quantification of area of fb and pb in a. (c) Skeletal preparation of *Pdgfra*$^{+/fl}$;*Mesp1Cre* and *Pdgfra*$^{fl/fl}$;*Mesp1Cre* at E18.5 (top view). Dashed lines outline fb and pb. (d) Quantification of area of fb and pb in c. (e) Micro CT scanning of *Pdgfra*$^{+/fl}$;*Wnt1-Cre2*, *Pdgfra*$^{fl/fl}$;*Wnt1-Cre2*, *Pdgfra*$^{+/fl}$;*Mesp1Cre* and *Pdgfra*$^{fl/fl}$;*Mesp1Cre* at E18.5 (side view). Red dashed lines represent section level in f. (f) Virtual sections of samples in e at marked level. fb, frontal bone; ip, interparietal bone; ob, occipital bone; pb, parietal bone. Scale bar = 1mm.

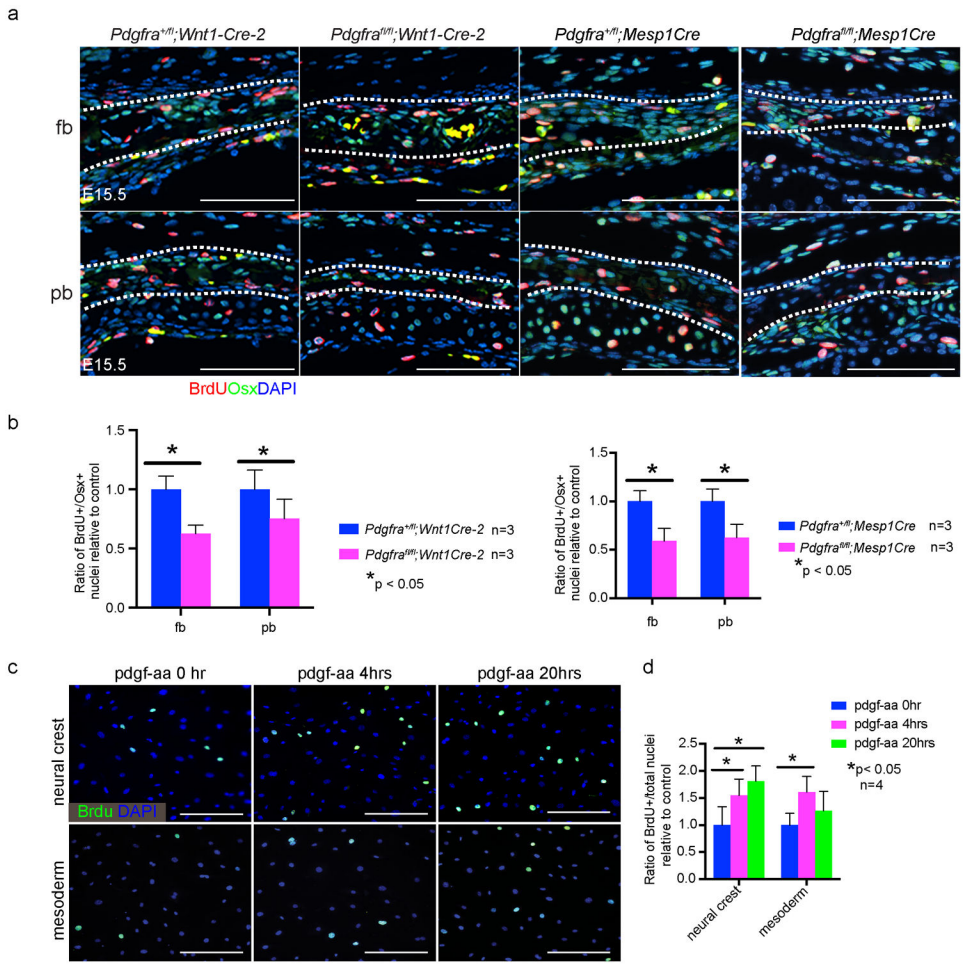

Figure 3. Analysis of Pdgfra regulated cell proliferation in vivo and in vitro.

(a) BrdU labeling (red) on transverse section of *Pdgfra*$^{+/fl}$*;Wnt1-Cre2*, *Pdgfra*$^{fl/fl}$*;Wnt1-Cre2*, *Pdgfra*$^{+/fl}$*;Mesp1Cre* and *Pdgfra*$^{fl/fl}$*;Mesp1Cre* at E15.5, counterstained with anti-Osx antibody (green) and DAPI (blue). (b) Quantification of BrdU labeling results in a. (c) BrdU labeling (green) of sorted tdTomato cells from E13.5 embryonic head counterstained with DAPI (blue). Neural crest cells are sorted from *Wnt1Cre-2;R26R*^{tdT} and mesoderm cells are sorted from *Mesp1Cre;R26R*^{tdT}. Cells were treated with pdgf-aa for 0 hr, 4hrs, or 20 hrs. (d) Quantification of BrdU+/DAPI+ nuclei in c. fb, frontal bone; pb, parietal bone. Scale bar = 100 um.

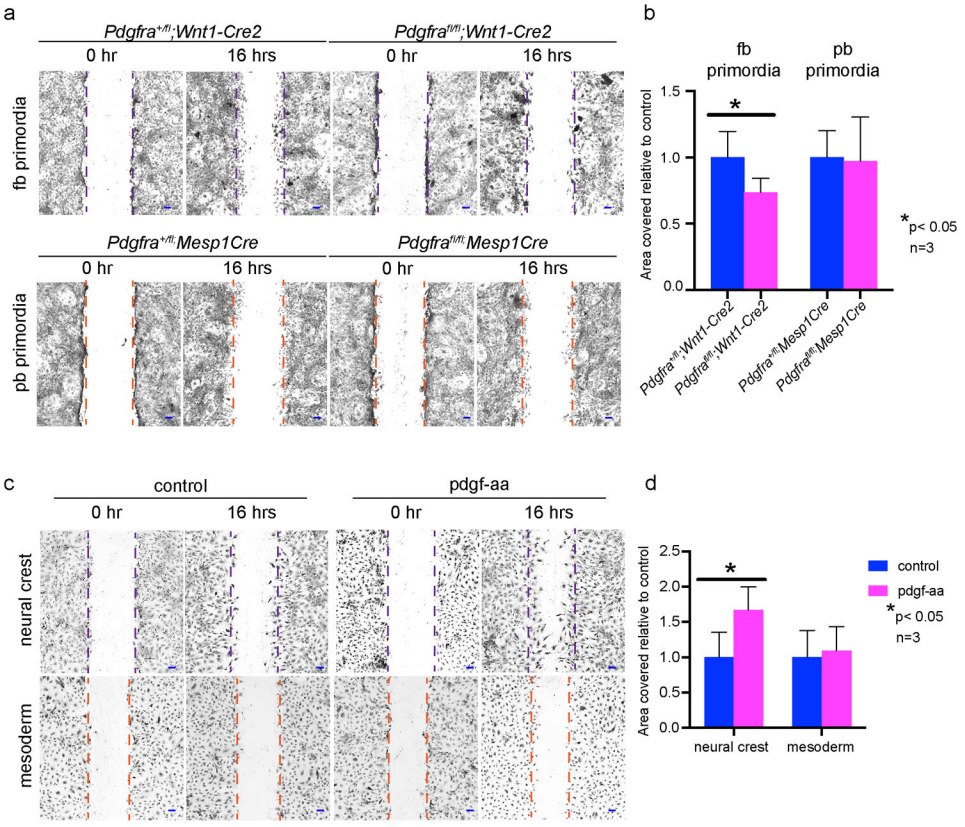

Figure 4. Analysis of Pdgfra regulated cell migration in vivo and in vitro.

(a) Scratch assay of primary culture of fb primordia and pb primordia from *Pdgfra*$^{+/fl}$*;Wnt1-Cre2*, *Pdgfra*$^{fl/fl}$*;Wnt1-Cre2, Pdgfra*$^{+/fl}$*;Mesp1Cre* and *Pdgfra*$^{fl/fl}$*;Mesp1Cre* embryos at E14.5. (b) Quantification of covered area in a. (c) Scratch assay of neural crest cells and mesoderm cells treated with pdgf-aa for 0 hr and 16 hrs. (d) Quantification of area covered by sorted cells in c. Scale bar = 100 um.

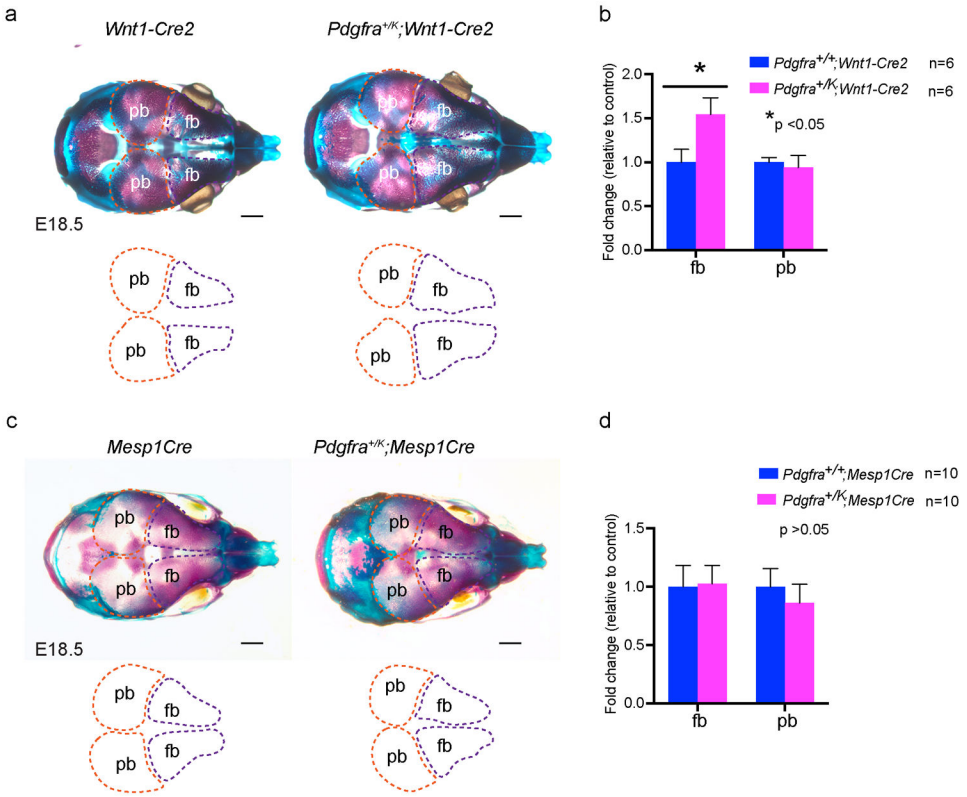

Figure 5. Activating Pdgfra in specific lineage causes differential calvarial phenotype

(a) Skeletal preparation of *Wnt1-Cre2* and *Pdgfra*$^{+/K}$*;Wnt1-Cre2* at E18.5 (top view). Dashed lines outline fb and pb of each embryo. (b) Quantification of area of fb and pb in a. (c) Skeletal preparation of *Mesp1Cre* and *Pdgfra*$^{+/K}$*;Mesp1Cre* at E18.5 (top view). Dashed lines outline fb and pb of each embryo. (d) Quantification of area of fb and pb in a. fb, frontal bone; pb, parietal bone. Scale bar = 1mm

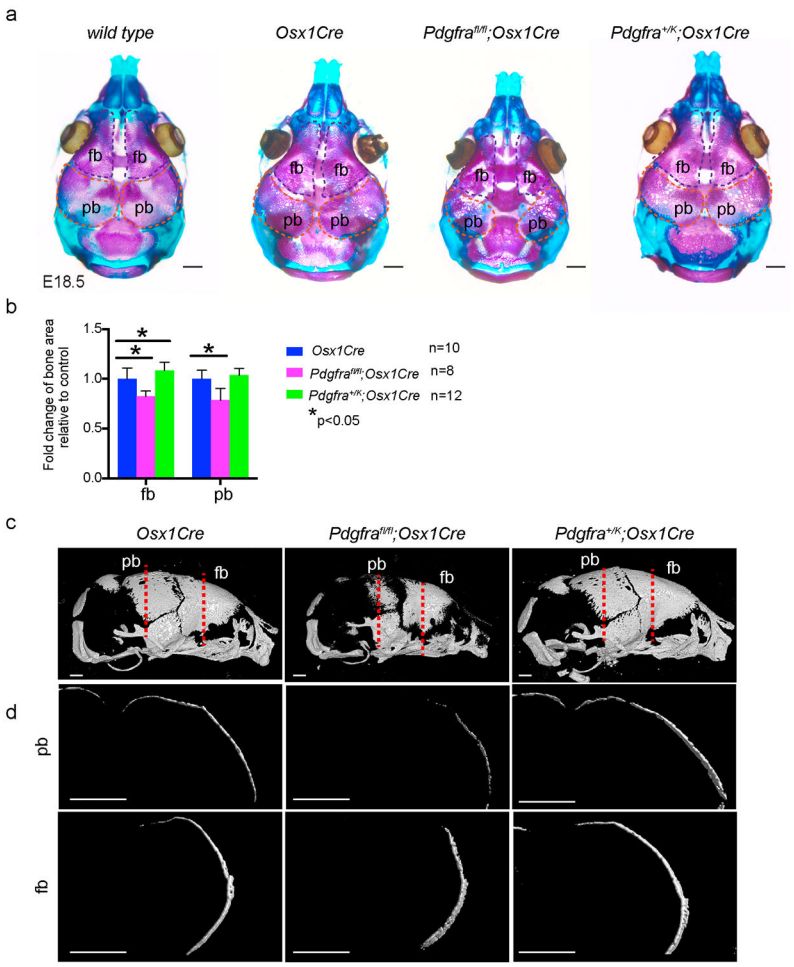

Figure 6. Osteoblast-specific manipulation of Pdgfra activity in calvarial development

(a) Skeletal preparation of *wildtype*, *Osx1Cre*, *Pdgfra*$^{fl/fl}$*;Osx1Cre* and *Pdgfra*$^{+/K}$*;Osx1Cre* at E18.5 (top view). Dashed lines outline fb and pb. (b) Quantification of area of fb and pb in a. (c) MicroCT scanning of *Osx1Cre*, *Pdgfra*$^{fl/fl}$*;Osx1Cre* and *Pdgfra*$^{+/K}$*;Osx1Cre* at E18.5 (side view). Red dashed lines represent section level in d. (f) Virtual sections of samples in c at marked level. fb, frontal bone; pb, parietal bone. Scale bar = 1mm.

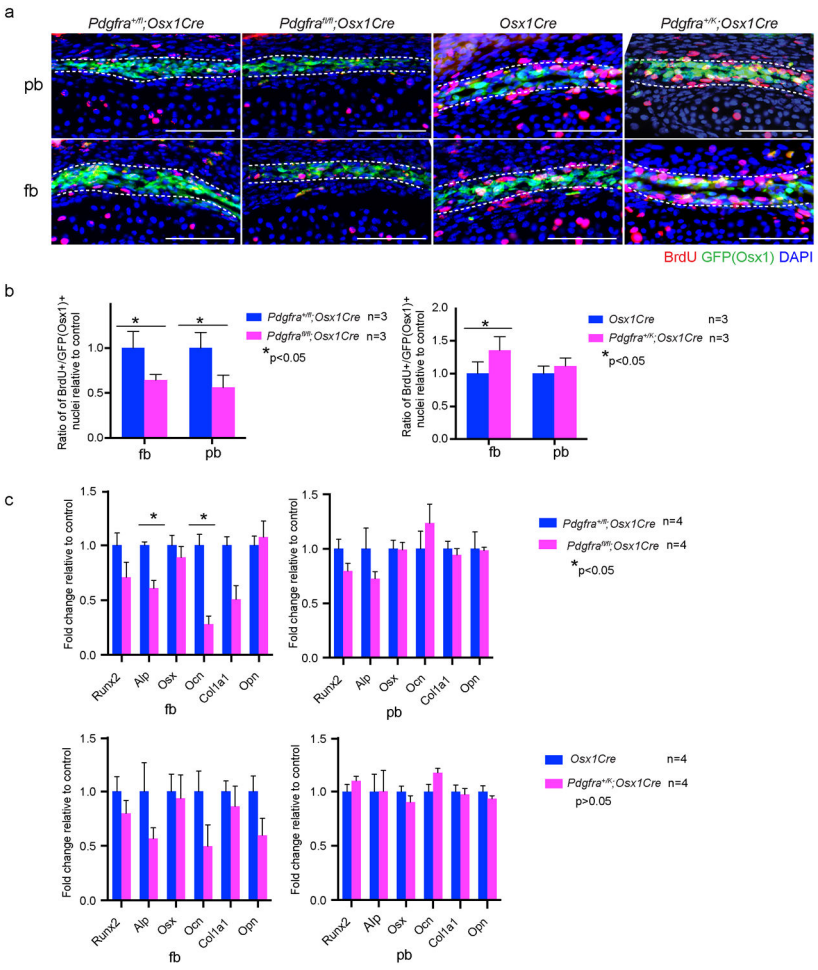

Figure 7. Analysis of Pdgfra regulated osteoblast proliferation and differentiation in vivo

(a) BrdU labeling (red) on transverse sections of *Pdgfra*$^{+/fl}$*;Osx1Cre*, *Pdgfra*$^{fl/fl}$*;Osx1Cre, Pdgfra*$^{+/+}$*;Osx1Cre* and *Pdgfra*$^{+/K}$*;Osx1Cre* counterstained with anti-GFP antibody (green, GFP is expressed by Osx1Cre transgenic allele) and DAPI (blue) at E15.5. (b) Quantification of BrdU+/GFP+ ratio in a. (c) Quantitative PCR result of marker gene expression in frontal bones and parietal bones of E18.5 *Pdgfra*$^{+/fl}$*;Osx1Cre* and *Pdgfra*$^{fl/fl}$*;Osx1Cre*, *Pdgfra*$^{+/+}$*;Osx1Cre* and *Pdgfra*$^{+/K}$*;Osx1Cre* embryos. fb, frontal bone; pb, parietal bone. Scale bar = 100 um.

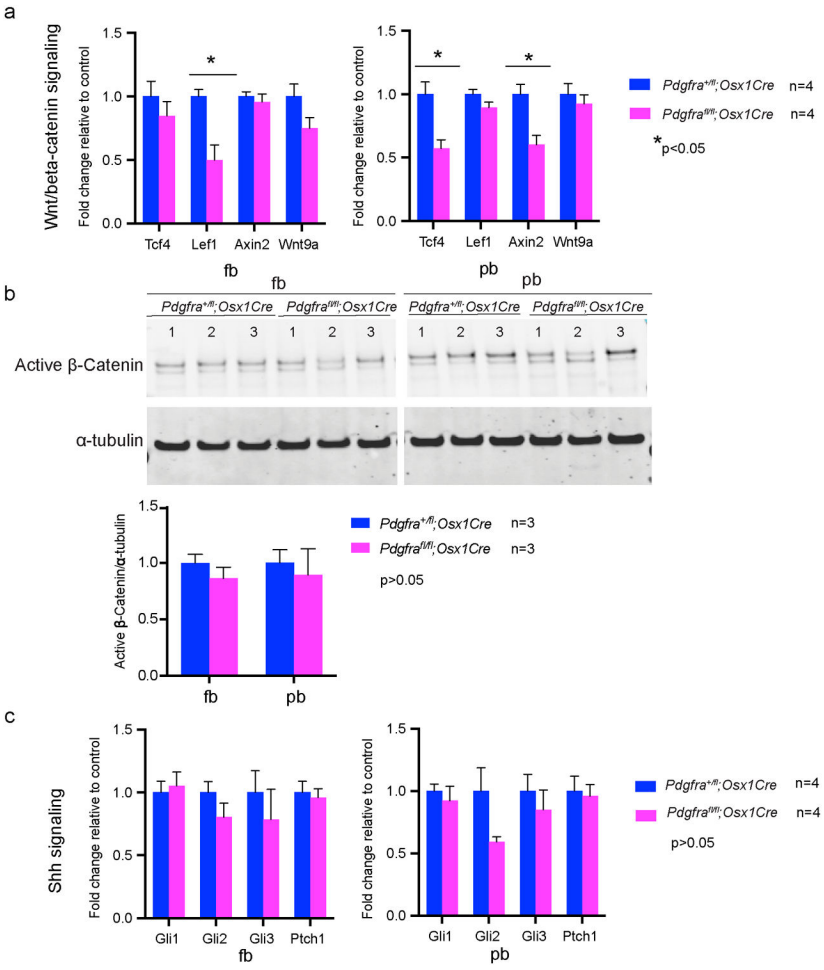

Figure 8. Examining crosstalk between Pdgfra and other signaling involved in calvarial development.

(a) Quantitative PCR result of Wnt/beta-catenin signaling target genes expression level in osteoblasts isolated from frontal bones and parietal bones of E18.5 *Pdgfra*$^{+/fl}$*;Osx1Cre* and *Pdgfra*$^{fl/fl}$*;Osx1Cre* embryos. (b) Western blot and quantification of active β-catenin and α-tubulin in lysates from fb and pb of E18.5 embryos. (c) Quantitative PCR result of Hh signaling target genes expression level in osteoblasts isolated from frontal bones and parietal bones of E18.5 *Pdgfra*$^{+/fl}$*;Osx1Cre* and *Pdgfra*$^{fl/fl}$*;Osx1Cre* embryos. fb, frontal bone; pb, parietal bone.